Materials Research. 2017; 20(1): 102-108
DOI: http://dx.doi.org/10.1590/1980-5373-MR-2015-0753
© 2017

Electrical and Optical Transport Characterizations of Electron Beam Evaporated V Doped In_2O_3 Thin Films

Md. Ariful Islam[a]*, Ratan Chandra Roy[b], Jaker Hossain[b], Md. Julkarnain[b], Khairul Alam Khan[b]

[a] Department of Physics, Rajshahi University of Engineering & Technology – RUET, Rajshahi, Bangladesh
[b] Department of Applied Physics & Electronic Engineering, University of Rajshahi, Rajshahi, Bangladesh

Received: December 8, 2015; Revised: August 24, 2016; Accepted: September 7, 2016

Vanadium (5 at. %) doped Indium Oxide (V: In_2O_3) thin films with different thicknesses (50 nm, 100 nm and 150 nm) were prepared onto glass substrate by electron beam evaporation technique in a vacuum of about 4×10^{-3} Pa. X-ray diffraction (XRD) pattern revealed that the prepared films of thickness 50 nm are amorphous in nature. Temperature dependence of electrical resistivity was studied in the 300 < T < 475 K temperature range. The films exhibit a metallic behavior in the 300 < T < 380 K range with a positive temperature coefficient of the resistivity (TCR), whereas at T > 380 K, the conduction behavior turns into a semiconductor with a negative TCR. Optical studies revealed that the films of thickness 50 nm possess high transmittance of about 86 % in the near-infrared spectral region. The direct optical band gap lies between 3.26 and 3.00 eV depending on the film thickness.

Keywords: *Transparent conducting oxide, Activation energy, Indium oxide, V: In_2O_3 Thin films, Optical band gap*

1. Introduction

Transparent conducting oxide (TCO) has become the essential part of the optoelectronic applications due to its excellent transparent and conductive properties. TCO has unique characteristics such as low electrical resistivity (< 10^{-3} Ω-cm) and high optical transmittance in the visible region (> 80 %) with a wide energy band gap (3.70 eV)[1-3]. Due to these combined unique properties, TCO has been used in a wide range of applications such as flat panel displays, photovoltaic cells, light emitting diodes, solar cells, barrier layers in tunnel junctions, and thin film transistor (TFT)[4-8].

Literature reports on TCO films revealed that some TCO thin films have interesting physical phenomena such as metal–semiconductor transitions (MSTs). These transitions occur at a wide temperature range and are observed in doped TCO thin films[9-15]. Among the various TCO thin films like ITO, CdO, ZnO, SnO_2, Indium oxide (In_2O_3) has been widely used in flat panel displays, opto-electronic modulators, liquid crystal displays, solar cells, architectural glasses and photovoltaic devices. A variety of electrical properties such as metallic, semiconducting, or insulating behavior can be obtained depending on its stoichiometric form (In_2O_3)[16]. The structural and opto-electrical properties of oxide materials like In_2O_3 thin films are highly influenced by doping impurities. The impurities like tin (Sn), zinc (Zn), gallium (Ga), copper (Cu), zirconium (Zr), erbium (Er), molybdenum (Mo) and titanium (Ti) have been doped to In_2O_3 to produce technologically useful materials and studied extensively by many researchers[17-23]. Compared to these dopants, vanadium is one of the interesting and suitable external dopant in our study because indium has a valence of three, and vanadium has a valence of five. In V: In_2O_3 samples, vanadium acts as a cationic dopant in the indium oxide lattice, which results in n-doping of the lattice by providing one or two electrons to the conduction band. If vanadium substitutes with indium, it provides free electrons into the lattice and the electrical conduction will increase but it also acts as a neutral impurity scattering center and decreases the electrical conduction when combined with interstitial oxygen atoms. Its smaller ionic radius (78 pm) compared with (94 pm) for In^{3+} causes local strains and enhance the formation of grain boundaries. A variety of deposition techniques have been used for the preparation of undoped and doped In_2O_3 films such as reactive thermal evaporation method, electro-deposition, radio frequency magnetron sputtering[24–27]. Li et al. reported a transparent conducting V: In_2O_3 thin films for hole injection in organic light-emitting devices (OLEDs) prepared by a modification-specific reactive thermal co-evaporation method, which shows a minimum electrical resistivity of 7.95×10^{-4} Ω-cm and good optical transmittance in the visible spectra range[24]. Recently, Seki et al. fabricated transparent V: In_2O_3 thin films for OLED by spray chemical vapor deposition[28] and found the minimum resistivity of 1.08 × 10^{-3} Ω-cm and average transmittance in the visible range of 84 %. V: In_2O_3 nanofibers can be used as a gas sensor at low temperature[29]. Although there have been a number of investigations on the structural, electrical and optical

* e-mail: arifapee19@gmail.com

properties of the above-mentioned doped In_2O_3 films, no systematic study has been paid on the electrical and optical properties using vanadium as a dopant.

In this article, vanadium (5 at. %) doped indium oxide (V: In_2O_3) thin films were prepared onto glass substrate by the electron beam evaporation technique. The influence of thickness on the electrical and optical properties of the V: In_2O_3 thin films were investigated.

2. Experimental details

Vanadium doped (5 at. %) indium oxide thin films were prepared onto glass substrate by electron beam evaporation technique in vacuum at ~ 3×10^{-4} pa from In_2O_3 powder (99.999 % pure) and vanadium powder (99.999 % pure) obtained from Aldrich Chemical Company, USA. Each material was weighted by an electronic balance (Mettler TOLEDO, AB 204) having a resolution of ± 0.0001 g. The percentage of composition was determined as[30]:

$$Weight\,\%\,V = \frac{w_V}{w_V + w_{InO}} \times 100\% \quad (1)$$

Where W_v and W_{InO} are the weight of V and In_2O_3, respectively. When the chamber pressure was reduced to 3×10^{-4} pa, deposition was started with beam currents 60 mA by turning on the low tension (LT) switch. The deposition rates of VIO thin films are about 12.5 nms^{-1}.

The thicknesses of the films were determined using interference Fizeau fringes method[31]. The electrical contacts required for resistivity measurements were made with silver paste (leading silver D-200) above the films. Structural property of the V: In_2O_3 film was carried out in a PHYLIPS PW3040 X'Pert PRO XRD System. X-ray diffractogram of the sample was recorded using monochromatic CuK_α radiation (λ=1.54187 Å), scanning speed 2 degree/min, starting from 8^0 and ending at 80^0. The surface morphology of the film was studied using in a HITACHI S-3400N Scanning Electron Microscopy (SEM) system.

Temperature dependent electrical resistivity (ρ) measurements were performed by Van-der-Pauw technique using a standard four-probe setup[32]. The electrical contacts were made in the four corners using silver paste (leading silver D-200) above the films. Resistance was measured by applying a current through the sample, and measuring the voltage by digital multi-meters (KENWOOD DL-711), respectively. The optical transmittance spectra of films were recorded from 300 < T < 1100 nm wavelength using a SHIMADZU UV- double beam spectrophotometer at room temperature. To determine the band gap of the V: In_2O_3 thin films optically, the plot of $(\alpha h\nu)^2$ vs. ($h\nu$) was drawn for direct allowed transition. The value of the band gap was determined for the tangent of these curves which intersect the energy axis.

3. Results and Discussion

3.1. Structural Properties

XRD pattern of the as-deposited V: In_2O_3 thin film with thickness of 50 nm is shown in Figure 1. In the absence of sharp diffraction peaks in the XRD pattern indicates that the film is amorphous in nature. Similar result was observed in e-beam evaporated indium tin oxide films[10].

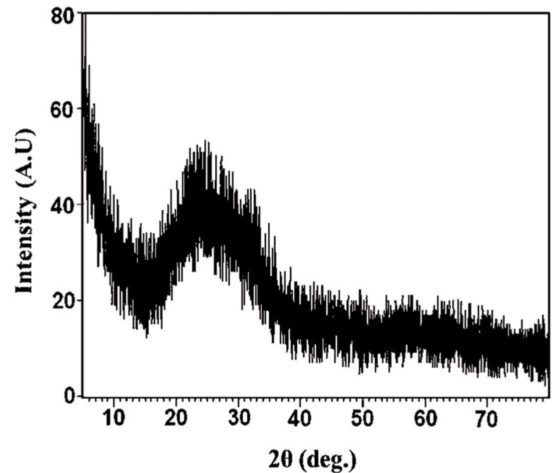

Figure 1: XRD pattern of the as-deposited V: In_2O_3 film with thickness of 50 nm.

Scanning Electron Microscopy (SEM) was used to study the surface morphology of V: In_2O_3 thin films. Figure 2 shows the SEM micrograph of the as-deposited V: In_2O_3 thin film with different thicknesses. The films display uniform morphology and possess nearly distributed grains over the surface.

3.2. Electrical properties

Figure 3 shows the resistivity versus temperature for a few typical V: In_2O_3 films with different thicknesses of 50 nm, 100 nm and 150 nm in the 300 <T < 475 K range. From Table 1 it is observed that the resistivity of V: In_2O_3 films strongly depended on the films thickness. At room temperature, the resistivity of the films decreases from 1.80×10^{-1} to 1.10×10^{-2} Ω-cm with increasing the films thickness. The decrease in resistivity with the films thickness may be attributed to the lesser relative contribution of the carrier scattering at the films surface[33]. Vanadium doping affects the resistivity of the V: In_2O_3 thin films. The minimum resistivity of 1.10 $\times10^{-2}$ Ω-cm is observed in V: In_2O_3 which is larger than that for pure indium oxide (~2.00×10^{-4} Ω-cm)[34] and indium tin oxide (~1.9×10^{-4} Ω-cm) thin films[35]. The reason for the increase in resistivity is that some V atoms may occupy interstitial positions and may also form defects such as V_2O

Figure 2: SEM micrograph of the as-deposited V: In_2O_3 film with different thicknesses.

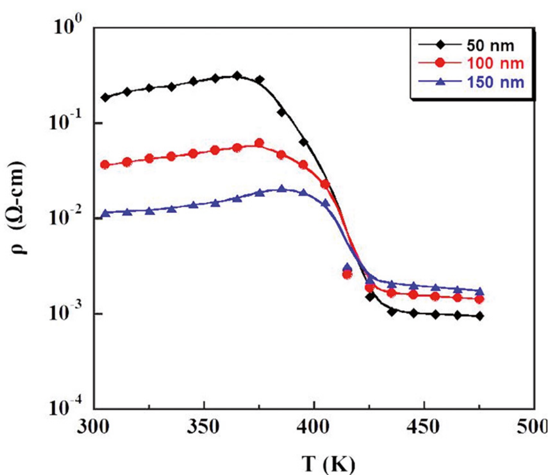

Figure 3: Temperature dependence of the resistivity (ρ) as a function of temperature (T) of V: In_2O_3 thin films with different thicknesses.

and V_2O_5, which acts as a carrier traps rather than electron donors. As observed from Figure 3, the resistivity for all films increases with increasing the temperature up to 380 K, showing metallic behavior. At approximately 380 K, the resistivity begins to decrease rapidly, and above 415 K, ρ decreases slowly with further increasing the temperature. The films display a semiconductor behavior at T > 380 K, and a minimum resistivity of 9.00×10^{-4} Ω-cm is found at 475 K. Metallic and semiconductor behavior are evidenced in the resistivity measurements as a function of temperature: a metal–semiconductor transition (MST).

The increase in resistivity with temperature is resulted mainly from a decrease in carrier concentration and Hall mobility. Some vanadium atoms may form point defect clusters which act as a carrier trap as explained above. The decrease in carrier concentration and mobility with increasing the temperature may be due to an increase in disorder of the crystal lattice, which causes phonon scattering and ionized impurity scattering and results in an increase in resistivity. At approximately 380 K, this point defect clusters are begun to rearrange and remove by small scale diffusion of Vanadium, thereby reducing in carrier scattering, consequently reducing the resistivity. Many theories have been developed to explain

Table 1: Dependence of resistivity on the films thickness at various temperatures.

No.	Thickness (nm)	Resistivity (Ω-cm)		
		At 300 K	At 380 K	At 475K
1	50	1.80×10^{-1}	3.30×10^{-1}	9.00×10^{-4}
2	100	3.60×10^{-2}	6.60×10^{-2}	1.40×10^{-3}
3	150	1.10×10^{-2}	2.10×10^{-2}	1.70×10^{-3}

defect removal during annealing[36-38]. Thus, rearrangement and elimination of point defect clusters leads to an increase in carrier concentration, thereby reducing resistivity.

Figure 4 shows that the films exhibit a positive TCR in the 300 < T < 380 K temperature range, whereas the films display a semiconductor behavior with a negative TCR in the 380 < T < 475 K range. The activation energy calculated from temperature dependent electrical conductivity measurements of V: In_2O_3 films. The plot of ln (σ) vs. 1000/T in the 380 < T< 475 K temperature range is shown in Figure 5. The plot is found to have two regions with two different slops with the point of inflection around 425 K. The presence of two regions with two different slopes in the plot may be due to the presence of two types of conduction in the V: In_2O_3 films, such as 380 < T < 425 K and above 425 K in the investigated temperature range. In the 380-425 K range, V may be provided electrons in the lattice which are activated to the localized state and this state moves toward the conduction band and thus increased conductivity. And above 425 K, impurity-impurity scattering may be increased which leads to decrease in the electrical conduction. Fitting the data using the linear equation:

$$\sigma = \sigma_0 \exp(-\Delta E/2K_B T) \quad (2)$$

where ΔE is the activation energy, σ_0 is the pre-exponential factor and K_B is the Boltzmann constant and T is the absolute temperature. In the 380 < T < 425 K temperature range, almost average ΔE of 8.25 eV is found, and at T > 425 K, ΔE is found to decrease from 0.40 to 0.20 eV with increasing the films thickness.

3.3. Optical properties

UV-VIS spectra of the films were studied using the optical transmittance measurements which were taken in the spectral region from 300 < *T* < 1100 nm. The variation of optical transmittance as a function of wavelength for V: In_2O_3 thin films with various thicknesses, as shown in Figure 6. It is seen from the figure that transmittance is greatly affected by films thickness, the thinner films of thickness 50 nm show relatively higher transmittance of about 86 % in the near infrared region. The films of thickness 100 nm are transparent with transmission of about 80 % and the thicker

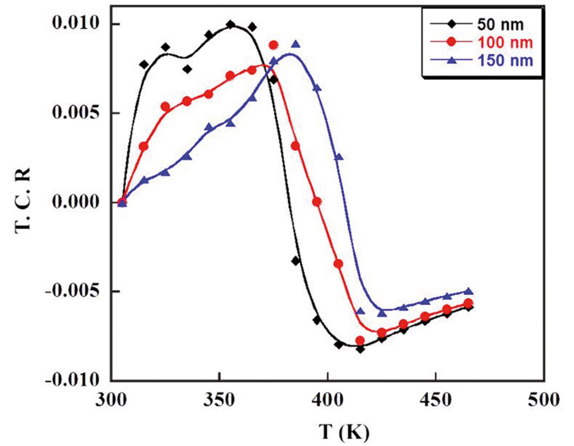

Figure 4: Variation of T.C.R. with temperature for the V: In_2O_3 thin films with different thicknesses.

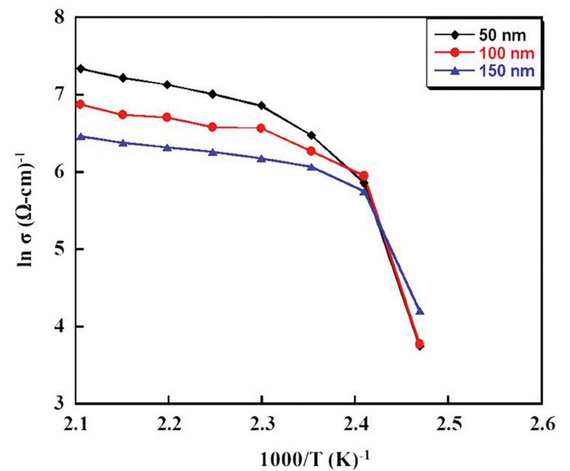

Figure 5: Plot of ln (σ) versus 1000/T of V: In_2O_3 thin films with different thicknesses in the temperature range 385-475 K.

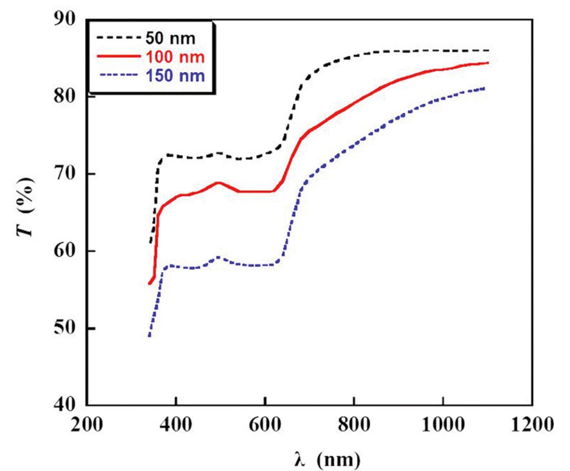

Figure 6: Spectral transmittance of V: In_2O_3 thin films as a function of wavelength with different thicknesses.

films of thickness 150 nm are relatively less transparent with transmission of about 75 % in the near infrared region. The reduction of transmittance with thickness may be attributed to the optical scattering arising from longer optical paths and also to changes in the carrier concentration[39,40]. In the visible region, transmittance of all films decreases sharply with decreasing the wavelength up to 620 nm, and after which, it remains almost constant with further increasing the wavelength up to 400 nm. This decrease of transmittance with the increase in photon energy is due to the absorption of free carrier.

The absorption coefficient (α) was calculated from the transmittance *(t)* using the relation[41]:

$$\alpha = 1/\mathrm{d}[\ln(1/T)] \quad (3)$$

where d is the film thickness and *T* is the transmittance. Figure 7 shows the variation of absorption coefficient with the photon energy (hv) of V: In_2O_3 thin films of different thicknesses. The absorption coefficient for all films is found to be the order of 10^4 cm^{-1}. The optical band gap (Eg) was determined from the absorption coefficient (α) and photon energy (hγ) using the following relation:

$$\alpha hv = A(hv - Eg)^m \quad (4)$$

where E_g is the optical band gap, hγ is the energy of the incident photon, and A is a constant and m takes the value of ½ and 2 for direct and indirect allowed transition, respectively. The direct allowed bang gap is obtained by plotting $(\alpha h\upsilon)^2$ against photon energy and extrapolating the linear part of the plots to zero absorption (α=0). Figures 8 (a)-(c) show the $(\alpha h\upsilon)^2$ versus (hυ) plots for various thicknesses. It is observed that E_g decreases from 3.26 eV to 3.00 eV with increasing thickness. This is possibly due to the increase in particle size and decrease in strain and dislocation density. The doping of vanadium into the indium oxide reduces the band gap (band gap of pure indium oxide is 3.75 eV[42]). This band gap reduction may be attributed to the decrease in carrier concentration because some V causes disorder in the indium oxide lattice and V atoms acts as a carrier trap instead of electron donors. This decrease in carrier density shifted the absorption edge towards lower energies. The band gaps of V: In_2O_3 films at various films thicknesses are inserted in Table 2. The resistivity, optical transmittance and direct band gap of the V: In_2O_3 thin films of the pervious works are compared in Table 3 with the present work.

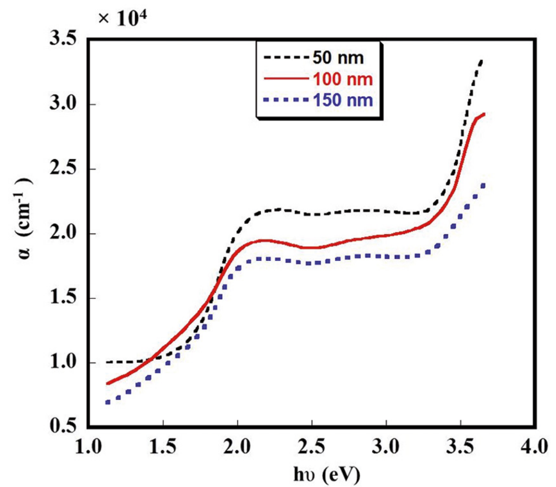

Figure 7: Absorption coefficient (α) as a function of photon energy (hυ) of V: In_2O_3 films with different thicknesses.

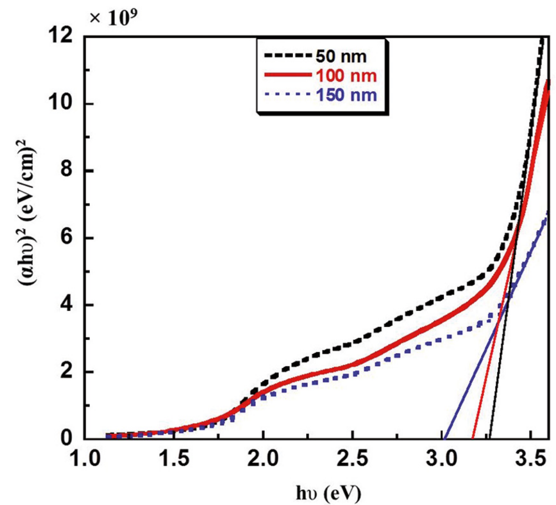

Figure 8: $(\alpha h\upsilon)^2$ versus photon energy (hυ) plots for V: In_2O_3 films with different thicknesses of (a) 50 nm, (b) 100 nm and (c) 150 nm.

Table 2: Optical band gap of V: In_2O_3 thin films with different thicknesses

No.	Thickness (nm)	AVT (%) (700-1000 nm)	Band gap (eV)
1	50	86	3.26
2	100	80	3.16
3	150	75	3.00

AVT average transmittance

4. Conclusions

Vanadium (5 at. %) doped indium oxide thin film was prepared onto glass substrate by electron-beam evaporation method. XRD analysis indicated that the V: In_2O_3 film is an amorphous one. Temperature dependent electrical resistivity were carried out in the 300 < T < 475 K temperature range. The films exhibit a metallic behavior with a positive TCR in the 300 < T < 380 K range. Semiconductor conductivity with metal-semiconductor transition is observed at T > 380 K in V: In_2O_3. For the film with 50 nm thickness, the resistivity value is close to 9.00×10^{-4} Ω-cm at 415 K and the transmittance is ~86 % in the near-infrared region. The optical band gap depends on the film thickness, which decreases from 3.26 to 3.00 eV. These

Table 3: Comparison of electrical and optical properties of V: In_2O_3 thin films with previous reported works of different TCO films by various techniques.

Technique	TCOs	(wt. %)	Thickness (nm)	ρ (Ω-cm)	AVT (%) (700-1100 nm)	E_g (eV)	Refs.
			50	1.80×10^{-1} (RT)	86	3.26	
E-beam	V:In_2O_3	5.0 % V	100	3.60×10^{-2} (RT)	80	3.16	Present work
			150	1.10×10^{-2} (RT)	75	3.00	
MSRTCE	V:In_2O_3	1.80 % V	-	7.95×10^{-4}	84	-	[24]
		3.05 % V		8.05×10^{-4}	84		
SCVD	V:In_2O_3	1.50 % V	-	1.10×10^{-3}	84	-	[28]
Thermal	Mo:In_2O_3	5.0 % Mo	-	5.20×10^{-4}	90	3.68	[17]
PLD	Sn:In_2O_3	5.0 % SnO_2	150	4.00×10^{-4}	85	3.89	[35]
			170	2.00×10^{-4}	92		
MOCVD	Ga:In_2O_3	0.1 % Ga	-	2.20×10^{-3}	78	3.89	[20]
		0.9 % Ga	-	1.90		4.46	
RF Sputtering	Ti:In_2O_3	2.5 % TiO_2	-	1.20×10^{-4}	75	-	[43]
ALD	Zr: In_2O_3		-	3.70×10^{-4}	-	-	[22]

MSRTCE modification-specific reactive thermal co-evaporation, SCVD spray chemical vapor deposition, PLD pulsed laser deposition, MOCVD Metal-Organic Chemical Vapour Deposition, ALD atomic layer deposition

structural, electrical and optical properties of V: In_2O_3 films are encouraging for application as a transparent conducting oxide and are suitable for many opto-electronic applications.

5. Acknowledgments

A. Islam is grateful to the Institute of Mining, Mineralogy & Metallurgy, BCSIR, Joypurhat, Bangladesh, for measuring the X– ray data. The authors also wish to thank Dr. Nuruzzaman and A. T. K. Karim for valuable discussions.

6. References

1. Dakhel AA. Optical properties of highly conductive and transparent Au-incorporated Eu oxide thin films. *Journal of Alloys Compounds*. 2009;470(1-2):195-198.

2. Meng Y, Yang X, Chen H, Shen J, Jiang Y, Zhang Z, et al. A new transparent conductive thin film In_2O_3: Mo. *Thin Solid Films*. 2001;394(1-2):219-223.

3. Xirouchaki C, Kiriakidis G, Pedersen TF, Fritzsche H. Photoreduction and oxidation of as-deposited microcrystalline indium oxide. *Journal of Applied Physics*. 1996;79(12):9349.

4. Ginley DS, Bright C. Transparent conducting oxides. *MRS Bulletin*. 2000;25(8):15-18.

5. Wagner JF, Keszler DA, Presley RE. *Transparent Electronics*. New York: Springer; 2008.

6. Fortunato E, Ginley D, Hosono H, Paine DC. Transparent Conducting Oxides for Photovoltaics. *MRS Bulletin*. 2007;32(3):242-247.

7. Chua BS, Xu S, Ren YP, Cheng QJ, Ostrikov K. High-rate room temperature plasma-enhanced deposition of aluminum-doped zinc oxide nano films for solar cell applications. *Journal of Alloys and Compounds*. 2009;485(1-2):379-384.

8. de Biasi RS, Grillo MLN. Influence of manganese concentration on the electron magnetic resonance spectrum of Mn^{2+} in CdO. *Journal of Alloys and Compounds*. 2009;485(1-2):26-28.

9. Naidu Muniswami RV, Subrahmanyam A, Verger A, Jain MK, Bhaskara Rao SV, Jha SN, et al. Electron-electron interactions based metal-insulator transition in Ga doped ZnO thin films. *Electronic Materials Letters*. 2012;8(4):457-462.

10. Liu XD, Jiang EY, Zhang DX. Electrical transport properties in indium tin oxide films prepared by electron-beam evaporation. *Journal of Applied Physics*. 2008;104(7):073711.

11. Nistor M, Perrière J. Metal–insulator transition in oxygen deficient Ti based oxide films. *Solid State Communications*. 2013;163:60-64.

12. Sun-Jian, Yang W, Huang Y, Lai WS, Lee AYS, Wang CF, et al. Properties of low indium content Al incorporated IZO (indium zinc oxide) deposited at room temperature. *Journal of Applied Physics*. 2012;112(8):083709.

13. Guo EJ, Guo H, Lu H, Jin K, He M, Yang G. Structure and characteristics of ultrathin indium tin oxide films. *Applied Physics Letters*. 2011;98(1):011905.

14. Lin BT, Chen YF, Lin JJ Wu CY. Temperature dependence of resistance and thermopower of thin indium tin oxide films. *Thin Solid Films*. 2010;518(23):6997-7001.

15. Li Y, Huang Q, Bi X. The change of electrical transport characterizations in Ga doped ZnO films with various thicknesses. *Journal of Applied Physics*. 2013;113(5):053702.

16. Bender M, Katsarakis N, Gagaoudakis E, Hourdakis E, Douloufakis E, Cimalla V, et al. Dependence of the photoreduction and oxidation behavior of indium oxide films on substrate temperature and film thickness. *Journal of Applied Physics*. 2001;90(10):5382.

17. Kaleemulla S, Madhusudhana Rao N, Girish Joshi M, Sivasankar Reddy A, Uthanna S, Sreedhara Reddy P. Electrical and optical properties of In_2O_3:Mo thin films prepared at various Mo-doping levels. *Journal of Alloys and Compounds*. 2010;504(2):351-356.

18. Ito M, Kon M, Miyazaki C, Ikeda N, Ishizaki M, Matsubara R, et al. Amorphous oxide TFT and their applications in electrophoretic displays. *Physica Status Solidi A*. 2008;205(8):1885-1894.

19. Moholkar AV, Pawar SM, Rajpure KY, Ganesan V, Bhosale CH. Effect of precursor concentration on the properties of ITO thin films. *Journal of Alloys and Compounds*. 2008;464(1-2):387-392.

20. Kong L, Ma J, Yang F, Luan C, Zhu Z. Preparation and characterization of $Ga_{2x}In_{2(1-x)}O_3$ films deposited on ZrO_2 (1 0 0) substrates by MOCVD. *Journal of Alloys and Compounds*. 2010;499(1):75-79.

21. Sasaki M, Yasui K, Kohiki S, Deguchi H, Matsushima S, Oku M, et al. Cu doping effects on optical and magnetic properties of In_2O_3. *Journal of Alloys and Compounds*. 2002;334(1-2):205-210.

22. Asikainen T, Ritala M, Leskelä M. Atomic layer deposition growth of zirconium doped In_2O_3 films. *Thin Solid Films*. 2003;440(1-2):152-154.

23. Ito N, Sato Y, Song PK, Kaijio A, Inoue K, Shigesato Y. Electrical and optical properties of amorphous indium zinc oxide films. *Thin Solid Films*. 2006;496(1):99-103.

24. Li H, Wang N, Liu X. Optical and electrical properties of Vanadium doped Indium oxide thin films. *Optics Express*. 2008;16(1):194-199.

25. Sharma R, Mane RS, Min SK, Han SH. Optimization of growth of In_2O_3 nano-spheres thin films by electro-deposition for dye-sensitized solar cells. *Journal of Alloys and Compounds*. 2009;479(1-2):840-833.

26. Peng LP, Fang L, Yang XF, Li YJ, Huang QL, Wu F, et al. Effect of annealing temperature on the structure and optical properties of In-doped ZnO thin films. *Journal of Alloys and Compounds*. 2009;484(1-2):575-579.

27. Sun SY, Haung JL, Lii DF. Effects of H_2 in indium–molybdenum oxide films during high density plasma evaporation at room temperature. *Thin Solid Films*. 2004;469-470:6-10.

28. Seki Y, Seki S, Hoshi Y, Uchida T, Sawada Y. Characteristics of vanadium-doped indium oxide thin films for organic light-emitting diodes fabricated by spray chemical vapor deposition. *Japanese Journal of Applied Physics*. 2015;54(4):041101.

29. Liu J, Guo W, Qu F, Feng C, Li C, Zhu L, et al. V-doped In_2O_3 nanofibers for H_2S detection at low temperature. *Ceramics International*. 2014;40(5):6685-6689.

30. Chopra KL. *Thin Film Phenomena*. New York: McGraw-Hill;1969.

31. Tolansky S. *Multiple Beam Interferometry of Surfaces and Films*. Oxford: Clarendon Press; 1948.

32. Van der Pauw LJ. A method of measuring specific resistivity and hall effect of discs of arbitrary shape. *Philips Research Reports*. 1958;13:1-9.

33. Giraldi TR, Escote MT, Bernardi MIB, Bouquet V, Leite ER, Longo E, et al. Effect of Thickness on the Electrical and Optical Properties of Sb Doped SnO_2 (ATO) Thin Films. *Journal of Electroceramics*. 2004;13(1):159-165.

34. Adurodija FO, Izumi H, Ishihara T, Yoshioka H, Motoyama M, Murai K. Influence of substrate temperature on the properties of indium oxide thin films. *Journal of Vacuum Science and Technology A*. 2000;18(3):814.

35. Kim H, Gilmore CM, Piqué A, Horwitz JS, Mattoussi H, Murata H, et al. Electrical, optical and structural properties if indium-tin-oxide thin films for organic light-emitting devices. *Journal of Applied Physics*. 1999;86(11):6451.

36. Primak W. Kinetics of Processes Distributed in Activation Energy. *Physical Review*. 1955;100:1677.

37. Meechan CJ, Brinkman JA. Electrical Resistivity Study of Lattice Defects Introduced in Copper by 1.25-Mev Electron Irradiation at 80°K . *Physical Review*. 1956;103:1193.

38. Damodara Das V. Modified equations for the evaluation of energy distribution of defects in as-grown thin films by Vand's theory. *Journal of Applied Physics*. 1984;55(4):1023.

39. Banerjee AN, Ghosh CK, Chattopadhyay KK, Minoura H, Sarkar AK, Akiba A, et al. Low-temperature deposition of ZnO thin films on PET and glass substrates by DC-sputtering technique. *Thin Solid Films*. 2006;496(1):112-116.

40. Agashe C, Kluth O, Schöpe G, Siekmann H, Hüpkes J, Rech B. Optimization of the electrical properties of magnetron sputtered aluminum-doped zinc oxide films for opto-electronic applications. *Thin Solid Films*. 2003;442(1-2):167-172.

41. Demichelis F, Kaniadakis G, Tagliferro A, Tresso E. New approach to optical analysis of absorbing thin solid films. *Applied Optics*. 1987;26(9):1737-1740.

42. Szczyrbowski J, Dietrich A, Hoffmann H. Optical Properties of RF-Sputtered Indium Oxide Films. *Physica Status Solidi A*. 1982;69(1):217-226.

43. Chaoumead C, Park HD, Joo BH, Kwak DJ, Park MW, Sung YM. Structural and Electrical Properties of Titanium-Doped Indium Oxide Films Deposited by RF Sputtering. *Energy Procedia*. 2013;34:572-581.

Materials Research.
DOI: http://dx.doi.org/10.1590/1980-5373-mr-2015-0753er

Erratum

In the article "*Electrical and Optical Transport Characterizations of Electron Beam Evaporated V Doped In_2O_3 Thin Films*", DOI number: http://dx.doi.org/10.1590/1980-5373-mr-2015-0753, published in Mat. Res., 20(1): 102-108, in the first page where it read:

Md. Ariful Islam[a] *

Ratan Chandra Roy[b]

Jakir Hossain[b]

Md. Julkarnain[b]

Khairul Alam Khan[b]

[a]Department of Physics, Rajshahi University of Engineering & Technology - RUET, Rajshahi, Bangladesh

[b]Department of Applied Physics & Electronic Engineering, University of Rajshahi, Rajshahi, Bangladesh

It should be written:

Md. Ariful Islam[a] *

Ratan Chandra Roy[b]

Jaker Hossain[b]

Md. Julkarnain[b]

Khairul Alam Khan[b]

[a]Department of Physics, Rajshahi University of Engineering & Technology - RUET, Rajshahi, Bangladesh

[b]Department of Applied Physics & Electronic Engineering, University of Rajshahi, Rajshahi, Bangladesh